

VOLUS—a visualization system for 3D ultrasound data

J. Varandas^a, P. Baptista^a, J. Santos^{b,*}, R. Martins^c, J. Dias^a

^a Department of Electrical Engineering and Computers, Institute of Systems and Robotics, University of Coimbra, polo 2, 3030-290 Coimbra, Portugal

^b Department of Electrical Engineering and Computers, Institute of Science and Materials Engineering, University of Coimbra, polo 2, 3030-290 Coimbra, Portugal

^c HUC, Hospital of University of Coimbra, Largo Mota Pinto, 3000-075 Coimbra, Portugal

Abstract

The main goal of this paper is the description of a computer based system for medical applications to estimate the half-ellipsoid model that fits the left ventricle on its two phases of cardiac cycle: diastole and systole. Techniques for registration and rendering of ultrasound images will be presented using 2D freehand spatial calibrated echocardiography images in order to represent the 3D reconstructed data equivalent to the scanned volume. The 3D reconstruction will be used to estimate and measure parameters of the half-ellipsoid model fitted to the left ventricle.

© 2003 Elsevier B.V. All rights reserved.

Keywords: Freehand 3D ultrasound; Calibration; Volume measurement; Medical imaging; Registration

1. Introduction

In last the three decades many researchers have attempted to produce systems which will allow the construction and visualization of three dimensional images from ultrasound data [1]. Currently, much pathology is diagnosed with the conventional equipment of ultrasound 2D.

The development of 3D ultrasonic systems offers additional benefits to the conventional systems. These include the acquisition and visualization of anatomy from different perspectives and measures of organs size and volume. In this article we present a system targeted for medical diagnosis and study of the left ventricle (LV) of the human heart. Three-dimensional ultrasonic systems have potential to reduce some existing errors in the 2D images such as the shade, spots known as speckle and reverberation.

The implementation of these technologies also enables to develop information fusion techniques to guarantee higher reliability of the data. The improvement of ultrasound 3D tends to supplant its inconveniences, and promote these systems as an essential tool in the several areas of application, including medical applications.

For the study of the left ventricle we developed a volumetric reconstruction process consisting of two phases: (1) identification of LV muscular mass extracted from the acquired B-scan images, and (2) filling up the voxels volume in accordance with the position and orientation of the B-scan ultrasound probe. To register the B-scans acquired during the sweeping of the human heart a previous geometric calibration of the hand-held system is performed. The method and the system apparatus is described in Section 3. A computational application, named VOLUS (VOLumetric Ultra-Sound), was developed to support the system use and its calibration.

2. Instrumentation development

The developed system (see Figs. 1 and 2) is composed by a magnetic DC tracking system and a position sensor (MiniBIRD® Model 500) attached to the ultrasound probe, producing high accurate data for the orientation and position of this probe. A frame grabber makes part of the system to acquire the B-scan images provided by the ultrasound equipment (ATL Ultrasound HDI 5000). The images are formatted with the Tagged Image File Format (TIFF) with a resolution 768 × 576 pixel. At the same time the position and orientation of the ultrasound probe are associated with each acquired image. The

* Corresponding author. Tel.: +351-239-796263.

E-mail address: jaime@deec.uc.pt (J. Santos).

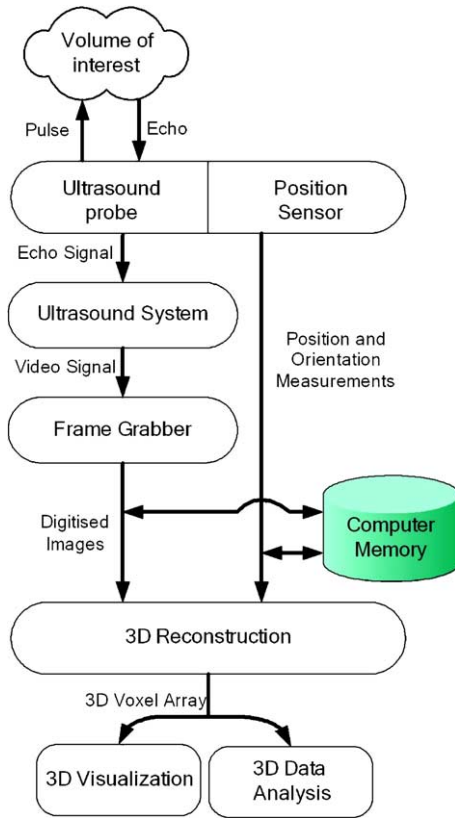


Fig. 1. Datapath of the system: acquisition, reconstruction, and visualization.

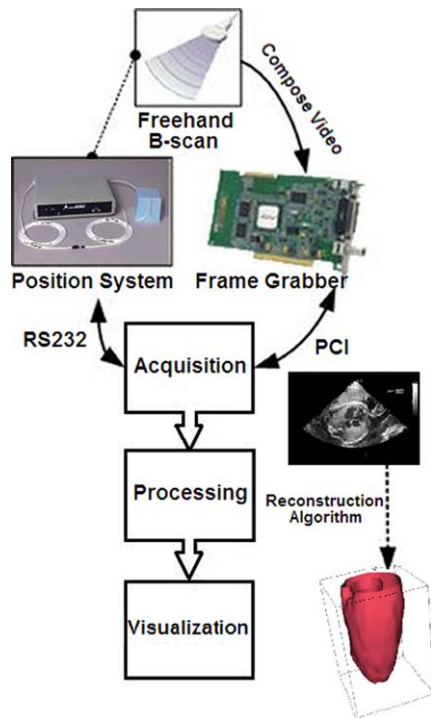


Fig. 2. Diagram of hardware and software components used on system.

position and orientation data are provided directly by MiniBIRD device via serial port RS232.

3. Geometric calibration

During the reconstruction and calibration, each a pixel of a B-scan image has to be registered in the reconstruction volumetric space. It is necessary to estimate the relation between the referential of the position sensor and the referential of the B-scan image (see Fig. 3). This requirement is known as geometric calibration, and it results on a set of eight parameters: three for position (x, y, z), three for orientation (α, β, γ) and two for image scaling (s_x, s_y).

In general, the calibration problem can be formulated as the following [2]:

$$m = {}^M T_O \cdot {}^O T_P \cdot {}^P T_I \cdot q, \tag{1}$$

with

$$q = \begin{bmatrix} s_x \cdot u \\ s_y \cdot v \\ 0 \\ 1 \end{bmatrix}, \tag{2}$$

where the matrix ${}^P T_I$ denotes the transformation from B-scan image coordinates frame $\{I\}$ to the position sensor on the ultrasound probe with coordinates frame $\{P\}$. The transformation ${}^O T_P$ describes the relation between the position sensor and MiniBIRD coordinate frame $\{O\}$. The transformation ${}^M T_O$ represents the relation from MiniBIRD coordinates to coordinate frame $\{M\}$ on the scanned volume. The variables u and v are the column and row indices of the pixel in the B-scan image (see Fig. 4), and s_x and s_y are the corresponding scaling factors ($mm/pixel$).

The coordinates of each a pixel are expressed in the coordinate system of the position sensor P (see Fig. 3) but they must be registered in the reconstruction volume with referential frame $\{M\}$. The matrix T illustrated in Eq. (3) represents the rigid body transformation from a

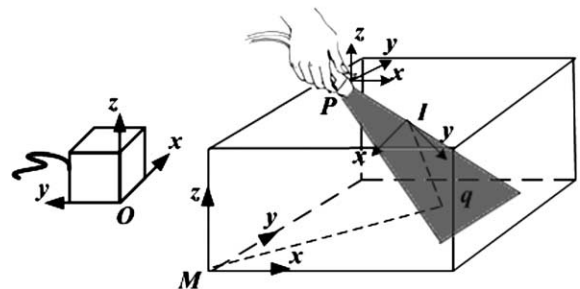


Fig. 3. Coordinate systems of the reconstruction and calibration process: image referential (I), position sensor referential (P), MiniBIRD referential (O), volume referential (M).

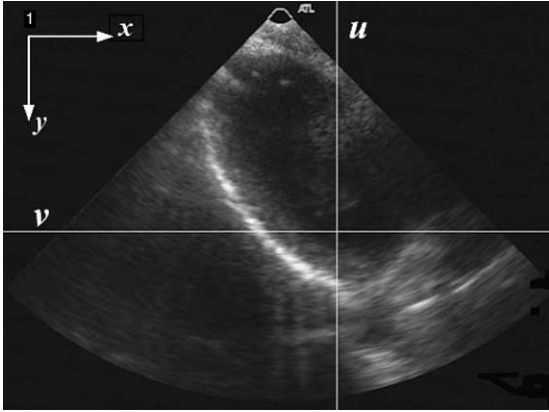


Fig. 4. B-scan image of the left ventricle: u and v represents the column and row of a pixel in the image referential (I), respectively.

generic coordinate system $\{J\}$ to generic coordinate system $\{K\}$:

$${}^K T_J(x, y, z, \alpha, \beta, \gamma) = \begin{bmatrix} c\alpha c\beta & c\alpha s\beta s\gamma - s\alpha c\gamma & c\alpha s\beta c\gamma + s\alpha s\gamma & x \\ s\alpha c\beta & s\alpha s\beta s\gamma + c\alpha c\gamma & s\alpha s\beta c\gamma - c\alpha s\gamma & y \\ -s\beta & c\alpha s\beta s\gamma & c\alpha s\beta c\gamma & z \\ 0 & 0 & 0 & 1 \end{bmatrix}, \quad (3)$$

where $c = \cos$ and $s = \sin$ were used for simplicity sake, the six degrees of freedom (α, β, γ) characterise the rotation and (x, y, z) the translation. The rotation between two coordinate systems is carried out by first rotating through γ around the x -axis, then through β around the y -axis, and finally through α around the z -axis.

The calibration consists of the estimation of matrix ${}^P T_I$, matrix ${}^M T_O$, and the coefficients s_x and s_y , according to Eq. (1). From the 14 unknown parameters only eleven will be identified for which, there are many possible methods. The used system device (see Fig. 5) is similar to the *Cambridge phantom* [3]. The technique is based on the scanning of the bottom of a container with water where each acquired B-scan image has one line that represents the intersection of the ultrasound beam with the bottom of the container. Assuming the bottom of the container is planar, all these lines are in the same plane and the coordinate system $\{M\}$ is defined at the level of the bottom of the container, with the z -axis exactly orthogonal to this, and then the pixels of the line have to satisfy the following equation:

$$\begin{bmatrix} x \\ y \\ 0 \\ 1 \end{bmatrix} = {}^M T_O \cdot {}^O T_P \cdot {}^P T_I \cdot \begin{bmatrix} s_x \cdot u \\ s_y \cdot v \\ 0 \\ 1 \end{bmatrix}. \quad (4)$$

In Eq. (4) the zero component can be written as a function of unknown parameters ϕ and measured the parameters θ as:

$$0 = f(\theta, \phi). \quad (5)$$



Fig. 5. Calibration device used for the calibration procedure.

For each a line in the image it is possible to select two pixels. That defines a line, thus providing two equations for each a B-scan.

The transformation ${}^O T_P$ is obtained directly from the MiniBIRD for each a B-scan. An initial estimation is given for the eleven parameters, which can be estimated using a classical optimization algorithm. Since the gradient of the function f in Eq. (5) can be easily computed by the Levenberg–Marquardt algorithm [3], this can be used to estimate the unknown parameters, using a minimum of eleven non-linear equations.

To evaluate the quality of the results, the root mean square error was calculated using a 3 MHz ultrasonic linear probe to indicate the convergence of the algorithm. A set of three calibration results are shown in Table 1.

Table 1
Calibration results

Parameter	Test 1	Test 2	Test 3
s_x (mm/pixel)	0.310	0.302	0.22
s_y (mm/pixel)	0.349	0.358	0.24
x_1 (mm)	4.9920	-6.0228	-3.455
y_1 (mm)	5.2330	0.0466	8.715
z_1 (mm)	-34.7965	-7.6191	-0.888
α (rad)	1.3172	-1.6510	-4.702
β (rad)	0.6401	-3.1723	3.135
γ (rad)	1.1677	0.5187	0.206
z_2 (mm)	-13.0898	12.0646	-11.244
β_2 (rad)	1.4440	4.6139	1.547
γ_2 (rad)	3.0900	2.7376	-3.794
B-scans	138	142	141
RMS error (mm)	0.35	0.42	0.85

4. Volumetric data visualization

There are several well developed techniques for rendering three-dimensional voxel data, including slicing, isosurface rendering, and volume rendering. These techniques are briefly described below.

The visualization process of the voxel is performed using the Visualization ToolKit (VTK) open source library, applied to B-scan images with 256 grey levels (see Fig. 6).

4.1. Slicing

In slicing, a plane is extracted from the voxels and displayed as a two-dimensional image. The slice may be either parallel to one of the axes of the voxels volume or at an arbitrary orientation. Clearly, a slice shows detailed information about the plane being displayed but it does not give an intuitive aspect of the LV. A simple and efficient method of visualizing the entire LV is to accomplish a sequence of slices, obtained by sweeping the cube parallel to one or more axes. The slice should be shown in perspective, in its correct position inside of the voxels volume, with a wire grid or set of axes to show the extent of it (see Fig. 7). The slice shows the intensity (grey levels) inside the voxel, which represents the different tissues and blood. The VOLUS application user is able to choose the position of these slices for better visualization.

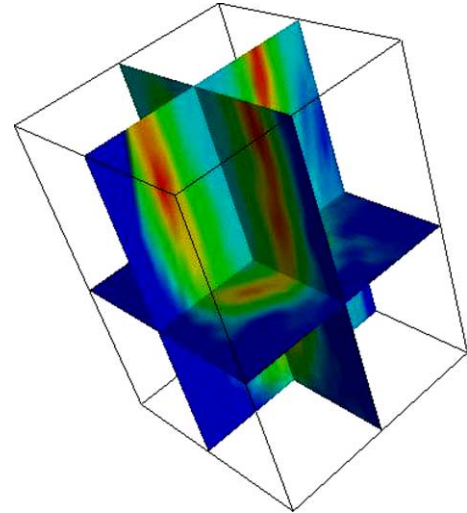


Fig. 7. 3D view of a slice in a voxel volume.

4.2. Isosurface

The visualization of surfaces is particularly challenging in freehand 3D ultrasound. In an isorendering, a so called isosurface corresponding to a given constant value within the data cube is computed and displayed. An isosurface is the three-dimensional analogy to the single contour in a two-dimensional pixel data set. Typically the isosurface will be displayed in perspective from a view point located at a small distance outside the

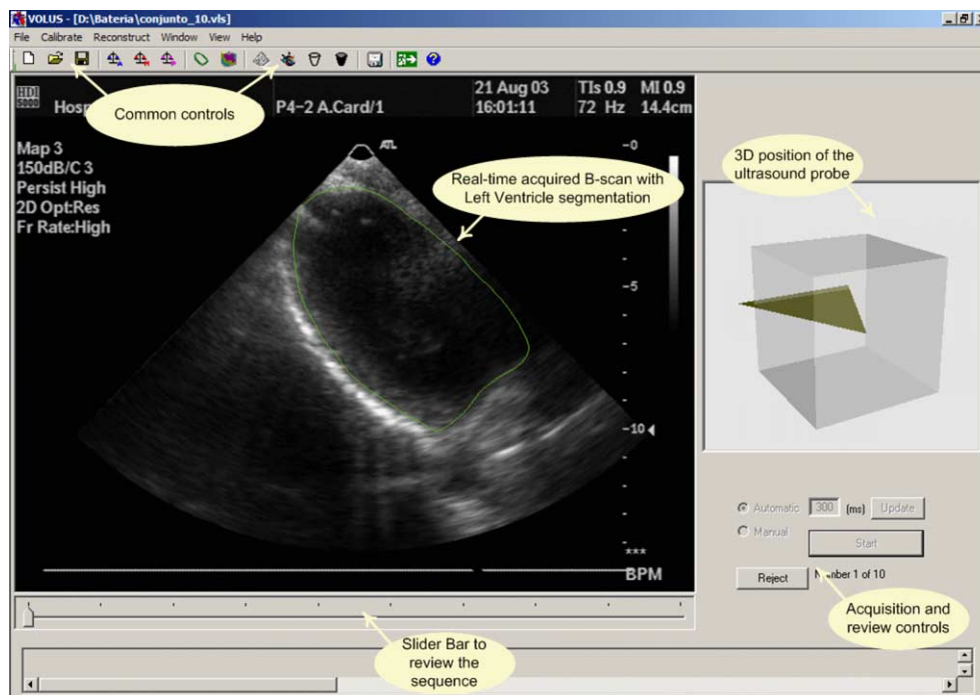


Fig. 6. VOLUS user interface. Simultaneous visualisation of the acquired B-scan and its spatial location.

voxel, and thus usually only one side of it will be visible (see Fig. 8). Extracting and displaying isosurfaces of volume data is useful in many areas. Three-dimensional (3D) data is clearly difficult to visualize, and rendering a surface within this data is one of the main techniques (though by no means the only one) available for this purpose. In addition to visualization, an extracted surface can also be used for measuring such as volume or surface area. A method of visualizing the entire voxel consists of the implementation of a sequence of isosurfaces sweeping from the lowest to the highest data values in the cube (or vice versa). Again the VOLUS user is able to define the value of the isosurface.

4.3. Volume rendering

Volume rendering is a technique for displaying an entire voxel without computing any intermediate surfaces. The result is an image like the one shown in the Fig. 9. Various algorithms for volume rendering have been proposed. Two common ones are ray-casting and splatting. Ray-casting was used in this work and is well explained in [4]. Splatting is similar to ray casting, though the details are more involved. It is quicker but produces less accurate results.

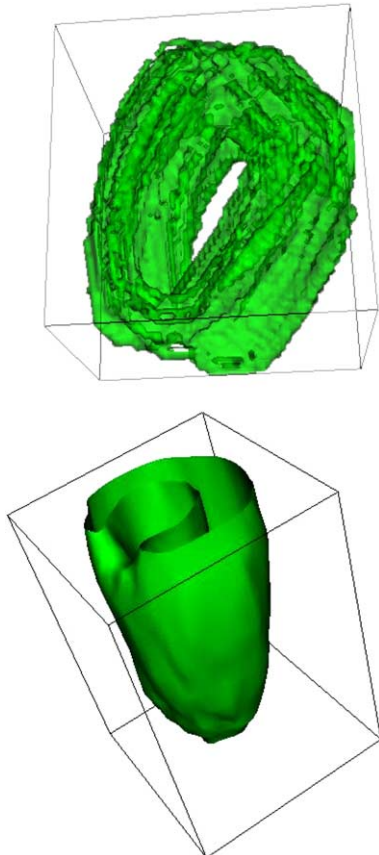


Fig. 8. 3D view of an iso-surface in a voxel volume.

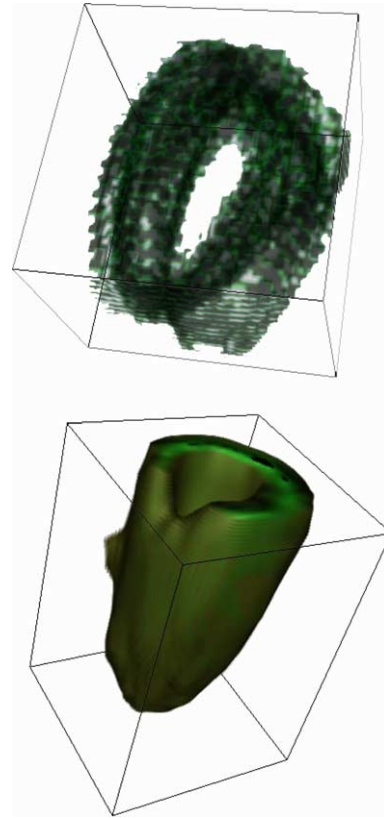


Fig. 9. 3D view of a volume rendering of a voxel volume.

5. Conclusion

At this point we have three processes accomplished: calibration, acquisition and visualization.

In the acquisition phase we observe that the Bscan's images are distorted by several noise sources including thermal noise from amplifying circuits, acoustic noise, phase effects (speckle noise and phase aberrations) depending on the probe type.

It is particularly important in freehand 3D ultrasound to acquire a good data set. This depends on both scanning technique and patient quietness. The latter is not an easy requirement to satisfy because of the heart dynamics, and the pressure of the probe carried out on the patient body. The doctor is able to visualize the data as the acquisitions are being made, in order to check if those requirements are satisfied.

The final results of our calibration process (as shown in Table 1) have higher precision when compared with the method using point based phantom, like the cross-wire and the three-wire [2], with the advantage that ours allow a reduced time in the image acquisition (about 3 min).

The calibration parameters are determined using an iterative registration algorithm between a plane phantom and two points of interest manually marked in 2D images.

We conclude that the 3D surface rendering has been useful for revealing high contrast structures. However multi-planar slice of the reconstructed grey level volume is useful for distinguishing genuine structure and is desirable in regions which are difficult to segment using a threshold level.

The utilization of this new fast evaluation method has provided an interactive system for designing surfaces and has demonstrated that may be of great interest in medical imaging.

6. Future work

To complete this work we are currently proceeding with the implementation of 3D reconstruction and 3D data analysis (volume measurement). Different mathematical models for ventricular volume are currently being tested, considering the heart's dynamics [5,6]. The development of semi-automatic voxel segmentation is an important to solve the problem since it will enable to extract clinically useful information from 3D ultrasound data.

In [7,8] is presented a recent study for assessment of left ventricular end-diastolic volume with freehand acquisition device and comparison with other medical diagnosis devices such as: Magnetic Resonance Imaging and gated single photon emission Computed Tomography. Both articles present clinical tests and discusses the advantages/disadvantages of free-hand devices. However no technical details about the image processing and mathematical models used during the tests are given. In our future work we intend to do similar clinical tests but studying the influence of different mathematical models and image data processing on the results. We believe

that any clinical assessment must be supported by the test of different technical options currently available for image processing and volume measurement.

References

- [1] T.R. Nelson, D.B. Downey, D.H. Pretorius, A. Fenster, *Three-Dimensional Ultrasound*, Lippincott Williams and Wilkins, 1999.
- [2] R.W. Prager, R.H. Rohling, A.H. Gee, L. Berman, *Automatic Calibration for 3-D Free-Hand Ultrasound*, Cambridge University Engineering Department, England, 1997.
- [3] W.H. Press, S.A. Teukolsky, W.T. Vetterling, B.P. Flannery, *Numerical Recipes in C++: The Art of Scientific Computing*, second ed., Cambridge University Press, 2002.
- [4] J.D. Foley, A. van Dam, S.K. Feiner, J.F. Hughes, *Computer Graphics, Principles and Practice*, Addison-Wesley Publishing Company, Massachusetts, 1992.
- [5] S. Hughes, T. D'Arcy, D. Maxwell, W. Chiu, A. Milner, J. Saunders, R. Shepard, Volume estimation from multiplanar 2d ultrasound images using a remote electromagnetic position and orientation sensor, *Ultrasound in Medicine and Biology* 22 (1996) 561–572.
- [6] S. Tong, H. Cardinal, R. McLoughlin, D. Downey, A. Fenster, Intra- and inter-observer variability and reliability of prostate volume measurement via two-dimensional and three-dimensional ultrasound imaging, *Ultrasound in Medicine and Biology* 24 (1998) 673–681.
- [7] H. Mannaerts, J. vand der Heide, T. Papavassiliu, J. Marcus, A. Beek, A. Rossum, J. Twisk, C. Visser, Quantification of left ventricular volumes and ejection fraction using freehand transthoracic three-dimensional echocardiography: comparison with magnetic resonance imaging, *Journal of the American Society of Echocardiography* 16 (2) (2003) 101–109.
- [8] J. Kawai, K. Tanabe, S. Morioka, H. Shiotani, Rapid freehand scanning three-dimensional echocardiography: Accurate measurement of left ventricular volumes and ejection fraction compared with quantitative gated scintigraphy, *Journal of the American Society of Echocardiography* 16 (2) (2003) 110–115.